COMPUTATIONAL MECHANICS AND PHYSICS AT NASA LANGLEY RESEARCH CENTER

Jerry C. South, Jr.
Chief Scientist
NASA Langley Research Center
Hampton, Virginia 23665

Abstract

An overview is given of Computational Mechanics and Physics at NASA Langley Research Center. Computational analysis is a major component and tool in many of Langley's diverse research disciplines, as well as in our interdisciplinary research. Examples are given for algorithm development and advanced applications in aerodynamics, transition to turbulence and turbulence simulation, hypersonics, structures, and interdisciplinary optimization.

Introduction

Research disciplines at Langley include aerodynamics, acoustics, structures, materials, electronics, controls, and atmospheric sciences. Computational analysis has become a dominant tool in most of these disciplines, providing enhanced insight into the physical processes that underlie our engineering and scientific problems. The use of computational analysis is so pervasive, and the expectations so great, that the demand by our researchers for more computer power seems insatiable. We have at our disposal a VPS-32 supercomputer (a 2-pipeline CYBER 205 with a 32 million, 64-bit word memory) in our central complex; access to a 4-pipeline 205 (with 8 million words of memory) in the Ames central facility; and of course, the NAS Cray-2. We have a parallel processor, a FLEX-32, which has 20 independent processors, each with 1 megabytes local memory and 2 megabytes shared memory. Additionally, there are a number of "super" minicomputers and over 100 other minicomputers sited in local research areas and associated printing and graphics terminals for pre- and post-processing computational results, and a local network for file transfers among the various resources.

In spite of what seems to be a considerable amount of computing power, we have saturated not only our VPS-32, but also "our half" of the Ames 205. As more codes are converted to CRAY FORTRAN or developed from scratch, we will saturate our share of the NAS as well (the usage rate as of this writing was about 300 hr/mo). This story is probably repeated at most research laboratories, and certainly many industries today, for several reasons. For example, nearly everyone seems to expect to make 7-hour runs on a supercomputer. The computations are usually three-dimensional simulations of physical problems and contain a wealth of detailed information not obtainable (or infeasible) by other means. Further, many more engineers and scientists are aware of, and use supercomputers in their research than was the case just 10 years ago. In the late 1960's, there were four supercomputers at Langley alone; namely CDC 6600's, which were ten times faster than their forerunners! However, it was almost unthinkable to make a 7-hour run, for the results of such a run would be so limited in use and would contain only a tiny fraction of the information compared to today's analyses.

We join with universities and industry to develop advances in computational methods for use in aerospace research. To assist in this thrust, the Institute for Computer Applications in Science and Engineering (ICASE) was created over 10 years ago at Langley to provide a direct interaction between university mathematicians and computer scientists and NASA research engineers to find an optimum blend among the theoreticians and the practitioners. The Institute has been an unqualified success. Mathematicians have been stimulated by association with difficult engineering problems, and research engineers have found the expertise of world-class numerical analysts, applied mathematicians, and computer scientists to be invaluable. A prime focus for ICASE researchers is development and analysis of computational algorithms for vector and parallel computers, such as the FLEX-32 mentioned previously.

In this paper an overview will be given of the algorithm developments and diverse applications of computational analysis at Langley which may be of interest to this conference. The main body of the paper is presented in the form of individual, self-contained briefs which were prepared by the researchers involved. It is intended that the briefs be as free of unexplained jargon and symbols as possible, in order to convey the scope of computational mechanics and physics at Langley, rather than exquisite details.

The majority of the briefs are in the area of computational fluid dynamics (CFD), as would be expected. Shown are examples of new Navier-Stokes and Euler equation algorithms for three-dimensional flows, and advanced viscous-inviscid computations using Euler and potential equations coupled with boundary-layer methods for three-dimensional aerodynamic problems. Some of the important CFD applications and developments in spectral methods coupled with Multigrid convergence acceleration are given. Vortex flows are a subject of intensive theoretical, computational, and experimental study at Langley, and some CFD applications are given here.

Researchers have developed CFD techniques for direct simulation of transition to turbulence, fully turbulent flows, and "large-eddy" simulations where the sub-grid scales of turbulent eddys are modeled. Both incompressible and compressible flows have been treated, and spectral methods are the predominant spatial differencing choice, due to the high accuracy of such schemes. This area of computational research consumes enormous computational resources, even for very simple geometry, and it has been one of our prime early focuses for NAS applications. Because transition and turbulence remain as a major stumbling block to the accurate prediction of complex flows, it continues to be a major research area at Langley, and NASA in

general. In another paper, M. Y. Hussaini presents a more comprehensive discussion of this area. Two examples of this research are shown in the main section.

The area of hypersonic flow is one which contains certain important problems that can be studied only by computational analysis, because of lack of experimental facilities capable of simulating the full range of hypersonic flight conditions. Hypersonics has been reborn as a top-priority engineering research field in the Nation, and NASA in particular, with the National Aero-Space Plane as a focus, along with advanced missions in support of our space program. Direct-simulation Monte-Carlo (DSMC) methods are used to explore and predict rarified flows, and to calibrate continuum Navier-Stokes codes which require slip boundary conditions at the solid walls of a vehicle. Finite-element and finite-difference methods are being developed for treating high-enthalpy, nonequilibrium flows and their interaction with structural elements. A significant focus area at Langley is the scramjet engine and its integration with the external aerodynamics of an Aero-Space plane, as regards spillage, combustion, and overall vehicle performance. The NASA hypersonic computational research will be covered in some detail in this conference in the paper by D. L. Dwoyer. Here we present one example in computational hypersonics, comparing Navier-Stokes, viscous-shock-layer, and DSMC algorithms for a rarified, nonequilibrium flow.

Computational structural mechanics at Langley is likely to become the fastest-growing community of supercomputer users. Structures researchers and designers in NASA and industry have developed and applied both linear and nonlinear finite-element methods with a high degree of sophistication for analysis of major problems in solid mechanics. The general software in use today evolved on computers with memory which was small relative to that available on current supercomputers; the solution techniques usually involve the generation of large linear systems of equations which are solved by some direct methods, such as elimination or inversion. The largest codes can require huge amounts of auxiliary storage, but are often relatively modest in terms of actual compute time (at least compared to CFD codes). Data generation and efficient input-output are a major concern. The NAS should be a particularly adept machine for such applications, for most problems which are presently analyzed will fit in the 256MW memory of the Cray-2. Static and dynamic analysis of large, complex structures, and fracture analysis of composite structures are two areas of research at Langley which require significant supercomputing resources, and the demand is growing rapidly. They are extremely well-suited for the NAS. Two examples of this work are shown in the following section, one of which relied on intensive use of the Cray XMP and Cray-2 at Ames via the NAS network to solve the analysis problem of the space shuttle solid-rocket booster joints. For this problem of national importance, the NAS network and its supporting personnel performed in admirable fashion.

The final example in the next section is one illustrative of our interdisciplinary research. A Langley research goal is to develop methods for integrating advances in our disciplines to achieve safer and more efficient aerospace vehicle and system designs. The example shown is a direct approach to maximizing electromagnetic performance of a large space antenna while minimizing the system mass.

Examples of Computational Analysis

Implicit Upwind-Biased Algorithm for Navier-Stokes Equations

An efficient computational algorithm for the compressible Navier-Stokes equations has been developed. The spatial differencing reflects the predominant nature of the equations in the limit of Reynolds number $R_e \to \infty$ (hyperbolic) and $R_e \to 0$ (parabolic) through upwind differencing of the convective and pressure terms and central differencing of the viscous shear stress and heat flux terms. The method is naturally dissipative so that no additional smoothing terms are required and is particularly well-suited for transonic and supersonic flows where strong shock waves are prevalent.

The algorithm is advanced implicitly in time by applying the backward-time Euler integration scheme to the governing equations, linearizing the equations in time, and using the delta form so that the steady-state solution is independent of the time step. Efficient solutions to the systems of equations are obtained at subsonic and transonic speeds through spatially split approximate factorization and at supersonic speeds through a hybrid relaxation/approximate-factorization technique. Extremely efficient solutions to the steady-state equations are obtained with multigrid acceleration.

Results from an example computation for the subsonic flow over an aspect ratio AR equal to one delta wing are shown in Figure 1. In this figure, Reynolds number based on length is represented by Re_L, free-stream Mach number by M_∞, lift coefficient by C_L, and trailing-edge flap angle by δ. The total pressure contours (shown in Fig. 2 at an angle of attack α of 20.5°) indicate the primary vortex, which is shed from the leading edge, and the secondary vortices (underneath the primary) which are induced by boundary-layer crossflow separation. The computation of lift versus angle of attack shows good agreement with experimental data and includes the prediction of maximum lift associated with the onset of vortex breakdown.

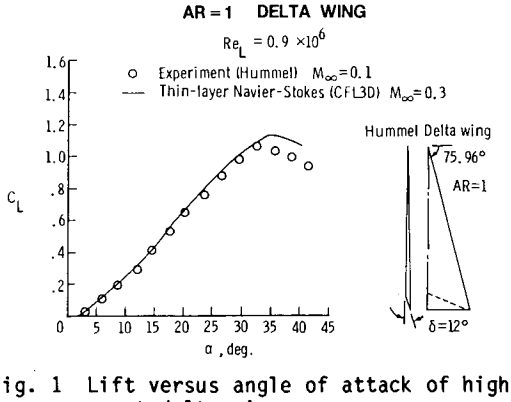

Fig. 1 Lift versus angle of attack of highly swept delta wing.

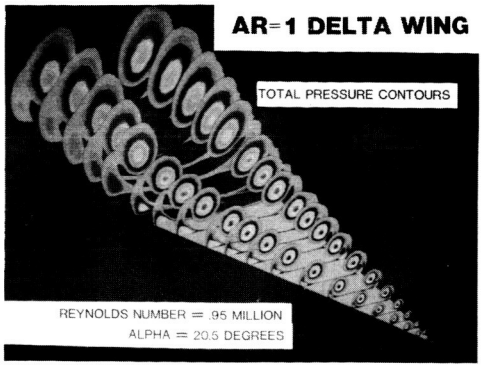

Fig. 2 Total pressure contours for highly swept delta wing.

Three-Dimensional Transonic Viscous-Inviscid Interaction Program

Over the past 5 years, the computer code TAWFIVE (Transonic Analysis of a Wing and Fuselage with Interacted Viscous Effects) has been under development at NASA Langley. The program was developed to accurately predict the transonic flow about wing-body configurations. In TAWFIVE, the conservative full-potential equation is used to model the outer inviscid portion of the flow field on a boundary-fitted grid. A three-dimensional integral boundary-layer method is used to model the inner viscous region of the flow field. Wake curvature and displacement thickness effects are also included.

The TAWFIVE code has recently been modified in an effort to significantly decrease its computation time and to add several new capabilities. Originally, TAWFIVE used a relaxation scheme to solve the outer inviscid portion of the flow. To accelerate convergence, the multigrid method has been incorporated. This method reduces total run times by at least 50%. Some improvements in the grid have also been made, and user input to the program has been reduced. Also, the capability to allow the wing lift level to be specified and the angle of attack to be a result of the calculation have been added.

As a sample of the capability of TAWFIVE, results from a TAWFIVE calculation for the Pathfinder I configuration are compared with experimental data from the National Transonic Facility. The flow conditions are $M_\infty = 0.82$, $\alpha = 1.93°$, and a Reynolds number R_e of 17×10^6 based on mean chord. Figure 3 shows good agreement for pressure coefficient C_p versus chord fraction x/c at three span fraction η locations.

Euler Code With Interacted Viscous Effects

An Euler code coupled with a boundary-layer solver has been developed by Keith Koenig, Mississippi State University, under contract to NASA. The code solves for the viscous flow field around a wing/fuselage combination. The finite-volume Euler solver uses flux-vector splitting of the governing equations and solves the discretized split equations with an implicit, upwind, second-

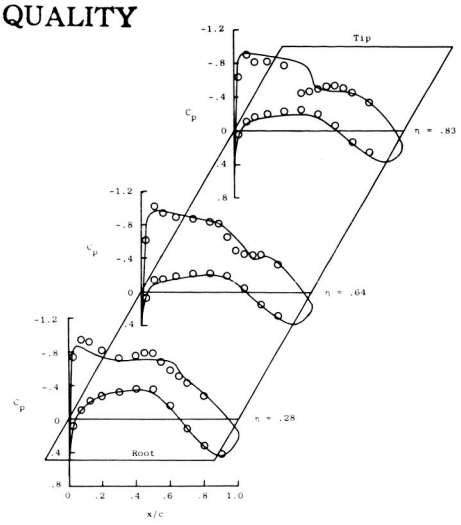

Fig. 3 Comparison of computational and experimental pressures for the Pathfinder I at $M_\infty = 0.82$, $\alpha = 1.93°$, $R_e = 17 \times 10^6$.

order predictor-corrector scheme. The viscous solver is an inverse integral technique that has analytical expressions for the velocity profiles which are valid for attached and separated turbulent boundary layers. The code is structured such that results can be obtained to engineering accuracy on the Control Data Corporation's VPS-32 computer in a DEBUG category run.

Results are presented for an advanced transport configuration at $\alpha = 2.41°$, $M = 0.819$, and $R_e = 5.9 \times 10^6$ and compared with experimental pressure coefficients at a midspan location on the wing. The computations were performed on a medium density C-H-shaped mesh (97×17×17). Comparisons of computed and experimental results on other configurations (including Pathfinder I) have also been made and are good. Plans are underway to apply the code to lower-aspect-ratio fighter-type configurations to further validate its capability.

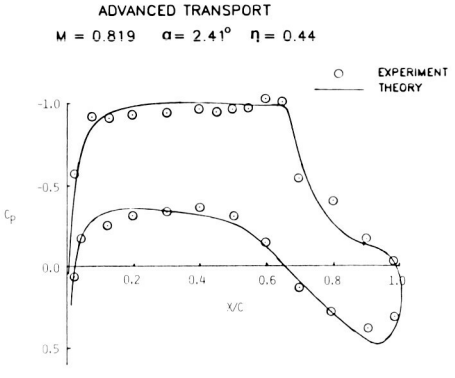

Fig. 4 Euler calculation with interacted viscous effects.

Aerodynamic Loads for Slender-Wing/Body Configurations

Low-aspect-ratio wings are desirable for vehicles that require supersonic or hypersonic capability, such as advanced fighter

configurations, missiles, or the proposed Aero-Space Plane. Due to their slender nature, these configurations exhibit substantial wing/body interference. In addition, separation-induced vortex flows naturally occur at moderate-to-high angles of attack and are dominant at conditions required for takeoff, landing, and maneuver. One theory that accounts for this flow, the free-vortex-sheet, has recently provided successful estimates, which include vortex-induced effects, of the surface load distributions for a slender configuration. Results from this theory are fully three dimensional and represent an inviscid "upper bound," which data tend to approach but not surpass as Reynolds number is increased.

A typical solution from the free-vortex-sheet theory is compared with experimental results in Figure 5 for a slender-wing/body configuration at an angle of attack of 20° and a free-stream Mach number of 0.5. The results are presented at a longitudinal station in which the body radius is approximately one-half of the configuration semi-span. Both theory and experiment show a double suction peak on the upper surface. The maximum pressure coefficient between these two peaks occurs at the wing/body juncture. The outboard suction peak occurs on the wing and is typical of leading-edge vortex flow; the inboard peak occurs on the fuselage and, for the theory, is solely due to induced effects of the wing primary vortex on the body.

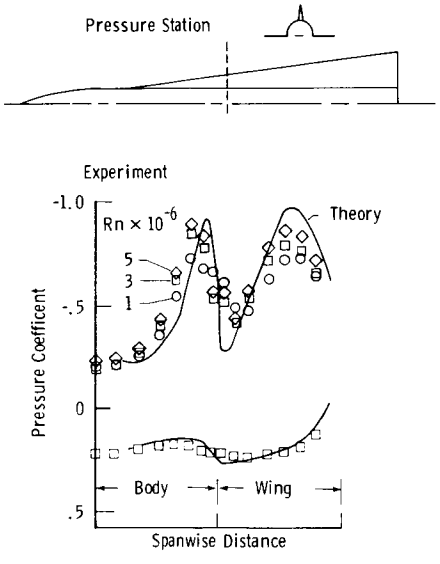

Fig. 5 Surface pressure correlation.

The correlation between theory and experiment is good on both the upper and lower surfaces. Similar correlations were achieved at other longitudinal stations. The experimental Reynolds number effects shown are significant, and, in this sense, the inviscid free-vortex-sheet theory may provide useful estimates of the full-scale flow that occurs at significantly higher Reynolds numbers than those shown.

New Algorithm Development for Efficient Transonic Unsteady Aerodynamic Analyses

An approximate factorization (AF) algorithm was developed at NASA Langley for solution of the unsteady small-disturbance potential equation for transonic flow. The new algorithm is very efficient for transonic unsteady aerodynamic and aeroelastic analyses when compared with the alternating-direction implicit (ADI) algorithm of the Air Force/Boeing XTRAN3S computer code. Figure 6 shows results of applications of the AF algorithm to an F-5 fighter wing. The free-stream Mach number was 0.9 and the angle of attack was 0°. A comparison of convergence histories of the AF and ADI algorithms is shown in the upper part of Figure 6.

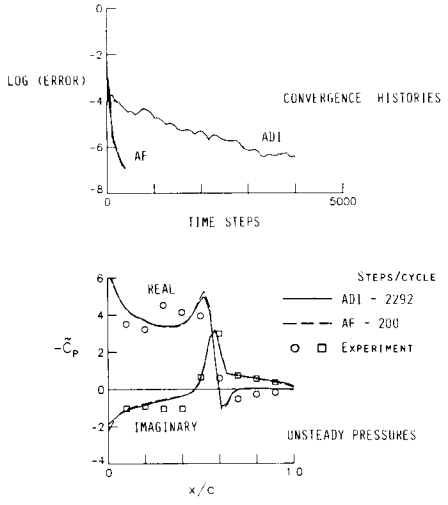

Fig. 6 Convergence histories and unsteady pressures.

The AF algorithm provides a converged steady-state solution in one-tenth the number of time steps that the ADI algorithm requires. The AF algorithm gives similar improvements in computational expense for subsequent unsteady calculations required for aeroelastic analyses. A comparison of unsteady pressure coefficients per unit pitch angle $\tilde{C}_p$, versus fractional chord at the wing midsemispan x/c, is shown in the lower part of Figure 6. The calculations were performed for the rigid wing pitching harmonically with a reduced frequency of k = 0.14. The AF results were obtained in a fraction of the number of time steps per cycle that the ADI results require, and both sets of results compare well with the experimental data. Therefore, the new AF algorithm is accurate and efficient for transonic unsteady aerodynamic analyses.

The research was conducted as part of a larger effort directed toward developing computational methods of predicting unsteady flows with emphasis on the flutter critical transonic speed range. In addition, the algorithm has been demonstrated to be effective in the supersonic regimes (not shown). Work is continuing to further assess the accuracy and efficiency of the new AF algorithm.

Automated Transonic Aeroelasticity Analysis Program Development

A procedure developed at NASA Langley for nonlinear transonic aeroelastic analysis of three-dimensional wings is based on the sequential and iterative use of a series of independent programs. For a fabricated wing shape, wing surface pressures are calculated using the FL022 aerodynamic program. A new wing shape resulting from the pressure loadings is then used in the next iteration. Three to six iterative loops are normally required to achieve convergence.

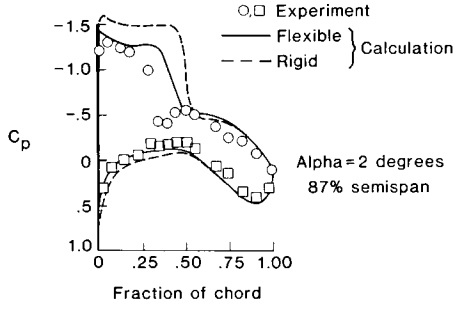

Fig. 7 Calculated and measured wing surface pressures.

Running the individual programs, transferring files, and evaluating intermediate results for a converged solution were found to be extremely time-consuming tasks. Linking programs, automating file transfers, and adding logic to exit the iterative loop when the convergence criteria were met have resulted in significant savings in user time and computer resources.

The automated procedure was used to provide results for comparison with experimentally measured data for a flexible transport-type wing tested in the Langley Transonic Dynamics Tunnel. Computed pressure coefficients for a rigid and a flexible wing show the calculated aeroelastic effects. The calculated pressure coefficients for the flexible wing agree well with the measured data, although the computed location for the recompression shock is slightly farther aft when compared with measured data. Also shown are computed and measured wing vertical deflections that are also in close agreement.

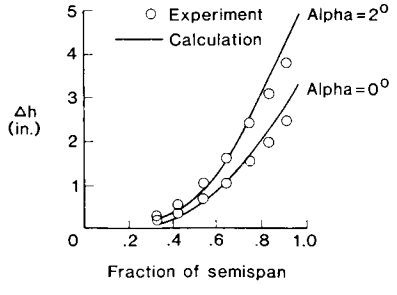

Fig. 8 Calculated and measured wing vertical deflections.

Transonic Airfoil Design Procedure

Transonic computational methods have matured to the point that they are being extensively used in the design of new configurations and the modification of existing aircraft. Their role in the design process has generally been to predict the flow field about a given configuration and to give the designer information about how changes affect the aerodynamic characteristics of the aircraft. More recently, automated design methods have been incorporated into some of the codes in an effort to expedite the design process.

A new algorithm at NASA Langley has been developed for use in the design of airfoils or wings that have a specified pressure distribution. This algorithm relates differences between the calculated and target pressure distributions to changes in airfoil surface curvature, then iteratively modifies the initial airfoil to achieve the desired pressures. This method works well for subsonic or transonic conditions because it accurately locates shocks when they are present, allows only a portion of the airfoil to be modified (if desired), and guarantees trailing-edge closure.

The Garabedian and Korn two-dimensional airfoil code has been modified to include this design procedure, and a number of test cases have been run at subsonic and transonic conditions. Results thus far indicate that the procedure is robust and accurate. An example of these results is shown in Figure 9. The target pressure coefficients were generated from an analysis run of the code for an existing supercritical-type airfoil at a Mach number of 0.734 and a lift coefficient of 0.60. The code was then run in the design mode using an NACA 0012 as the initial airfoil. At these conditions, both the initial and final pressure distributions show a considerable amount of supercritical flow on the upper surface terminating in a shock. The final pressure distribution for the modified airfoil was very close to the target pressure distribution.

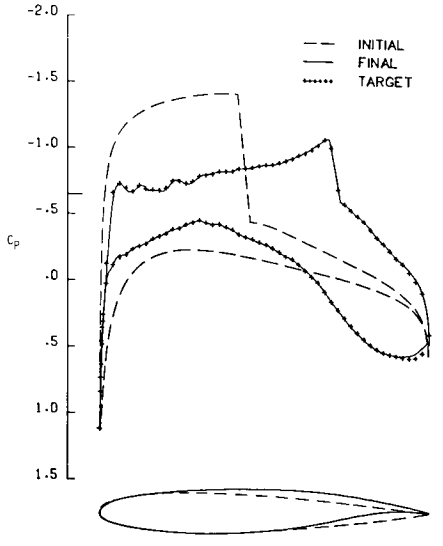

Fig. 9 Airfoil design code pressure distributions C_p.

Multiple-Domain Extension to Spectral Collocation Methods

Spectral collocation methods have proved to be efficient discretization schemes for many aerodynamic and fluid mechanic problems. The high-order accuracy shown by these methods allows either engineering-accuracy solutions on coarse meshes or, alternatively, very accurate solutions that are essential for fluid mechanic simulations. One drawback to spectral collocation has been the requirement that a complicated physical domain must be mapped onto a simple computational domain via a high-order mapping if the spectral advantages are to be preserved. Additionally, problems with discontinuous boundary conditions cannot be treated with conventional spectral methods. Such restrictions are overcome by splitting the domain into regions; adjoining regions are interfaced by enforcing a global flux balance that preserves the high-order continuity of the solution.

This multidomain method has proved to be effective on a wide range of test problems, which include resolution of a singular perturbation problem with spatial scales different by 5 orders of magnitude, and an elliptic equation in generalized nonorthogonal curvilinear coordinates. Figure 10 shows the solution isolines for Laplace's equation in a region that contains a line of fixed conditions within the domain. This discretization will be used in the simulation of transition in the shear layer behind the trailing edge of a splitter plate.

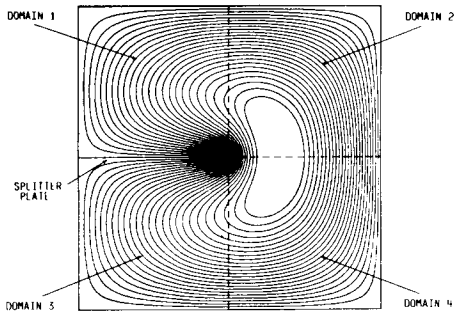

Fig. 10 Solution to Laplace's equation on splitter plate geometry.

Application of Spectral Multigrid Methods to Engineering Calculations

The high-order error decay rate that is associated with spectral methods can be used to an advantage in multidimensional engineering calculations by reducing the rapid growth in the number of points required by even modest increases in accuracy. To realize this advantage, however, efficient solution techniques must be devised to solve the equations that result from spectral discretization; these equations tend to be far more difficult to solve than the corresponding finite-difference equations. A number of techniques have been applied to spectral methods with considerable success. One such method involves preconditioning the spectral equations with a solution to the corresponding finite-difference equations and computing, at each step, the iteration parameters that yield fastest convergence. Preconditioning is a classical technique in which an algebraic system, which is to be solved iteratively, is modified by the inverse matrix of a related system which is easier to solve. This preconditioning clusters the eigenvalues of the system and results in faster convergence. Another powerful technique that has been employed is the well-know multigrid method. In this method, convergence is accelerated by taking advantage of the characteristic that is inherent in most relaxation schemes: convergence is rapid for short-wavelength error components, but it is slow for long-wavelength components. Relaxation solutions of related equations (written on a sequence of progressively coarser grids) are used to remove the entire error spectrum because a long-wavelength error on a fine grid appears as a short-wavelength error on a coarse grid.

An example of a solution that is produced by a spectral multigrid technique is shown in Figure 11, which illustrates the Mach number contours about a transonic shock-free airfoil. Simulation of shock-free transonic flow presents a severe test of the accuracy of a method. Low-accuracy flow field solutions often bear little resemblance to the true solution because nearly sonic flow is extremely sensitive to small area changes in the stream tubes. The equations produced by the spectral discretization of the potential equation could not be solved for this example by any other iterative method than the multigrid method.

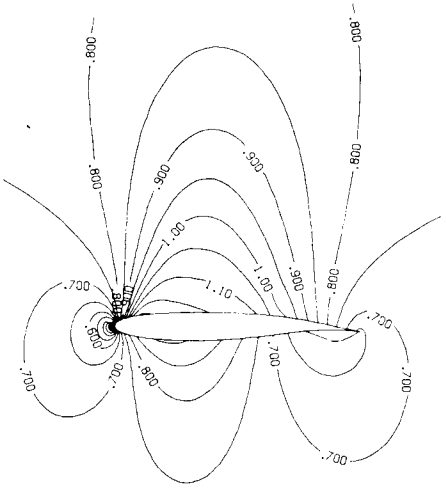

Fig. 11 Mach contours about a shock-free transonic airfoil.

Numerical Simulation of Boundary-Layer Transition

Spectral algorithms are used to conduct time-dependent, three-dimensional Navier-Stokes simulations of transition in idealized, parallel boundary layers. For incompressible water boundary layers, simulations are conducted both with and without passive wall heating in order to assess the effectiveness of this control mechanism in the strongly nonlinear regime. For compressible air boundary layers, the simulation is conducted at a free-stream Mach number of 4.5 in order to determine the influence of nonlinear, three-dimensional effects on compressible transition.

The numerical simulations indicate that wall heating can delay the transition process. One of the clearest diagnostics of the transition process is the development of a strong detached shear layer, i.e., a region (removed from the wall) in which the streamwise velocity has a high gradient in the direction normal to the wall. Figures 12(a) to 12(c) compare the flow field in an uncontrolled water boundary layer with that in one in which the wall has been heated to 2.75% above the free-stream temperature. After a nondimensional time of 3, the uncontrolled boundary layer has a strong detached shear layer, whereas the heated case still exhibits only a small perturbation to the mean flow.

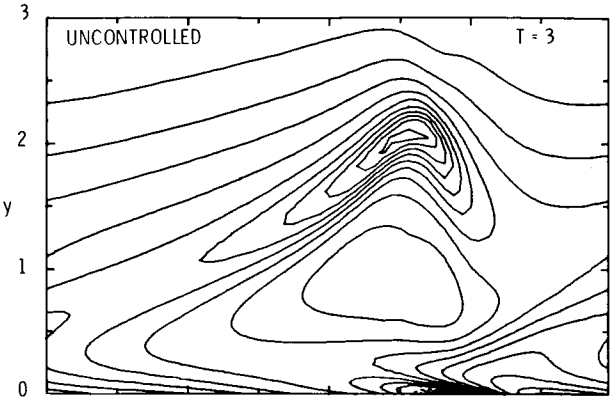

Fig. 12(a)

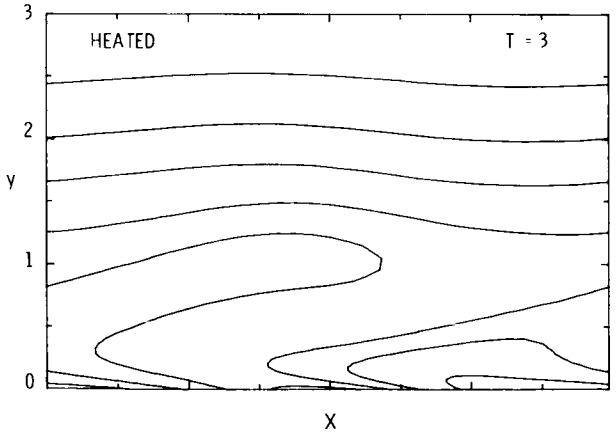

Fig. 12(b)

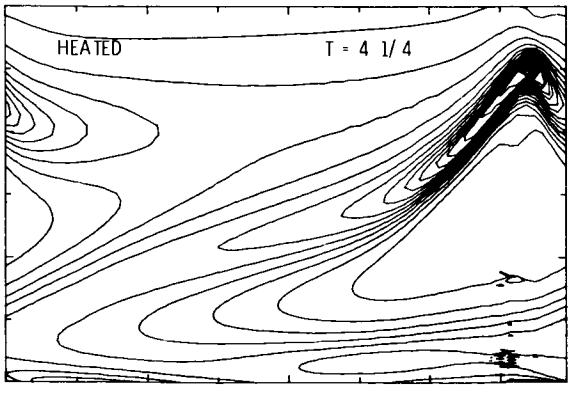

Fig. 12(c)

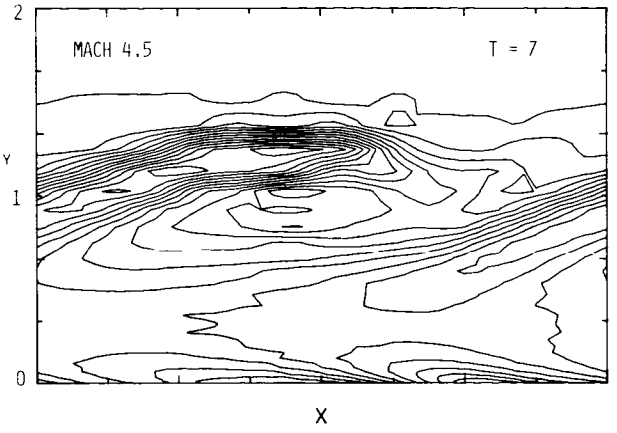

Fig. 12(d)

However, after a time of 4-1/4 even the heated case is undergoing transition. Wall heating delays transition but does not prevent it. The simulations of compressible flow have yielded the first theoretical evidence that nonlinear, secondary instabilities operate in the supersonic regime. Figure 12(d) presents a detached shear layer arising from a secondary instability in supersonic flow.

Subgrid-Scale Modeling of Compressible Turbulence

Highly accurate, spectral codes for both direct and large-eddy simulations of compressible, homogeneous turbulence were developed. The direct simulation (DS) code was used to generate fully resolved, low Reynolds number turbulent flow fields on 96×96×96 and 128×128×128 grids. The computed flow fields were separated, via a large-eddy simulation (LES) filtering process, into resolved and unresolved (subgrid) components with respect to both 16×16×16 and 32×32×32 grids. The subgrid-scale model was applied to the resolved fields to produce predictions for the subgrid-scale stresses. These were then compared with the exact subgrid-scale stresses as determined from the DS data. This comparison was used to find the optimal model constants and to compute the correlation between the modeled and exact subgrid-scale stresses.

A new subgrid-scale model for compressible turbulence has been developed and tested. It satisfies basic physical principles, includes compressibility effects, and can be implemented efficiently within an LES code. The DS and LES codes employ a novel, semi-implicit treatment of the pressure that permits efficient computation of very low Mach number flows. Direct simulations have been performed for Mach numbers (based on the rms value of the fluctuating velocity field) between 0.1 and 0.6. Figure 13(a) compares the energy spectrum for the Mach 0.6 case with a comparable spectrum for an incompressible case. Figure 13(b) illustrates the density fluctuations in the compressible case. Detailed data analysis has revealed that the compressible subgrid-scale model correlates well with the data, with correlations on the tensor level which are above 80%. Moreover, the constants in the model have only a weak dependence upon Mach number, changing by no more than 5% between Mach 0 and Mach 0.6.

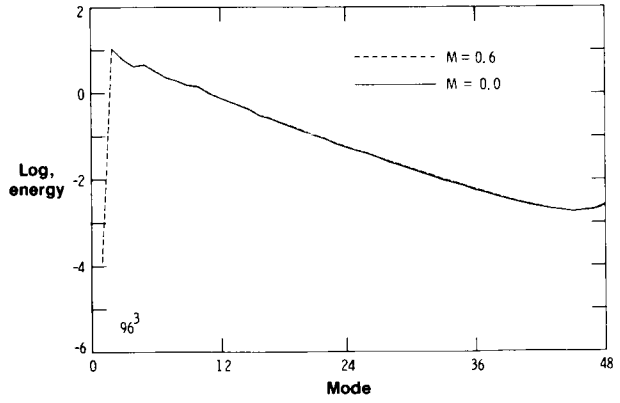

Fig. 13(a) Energy spectrum for isotropic turbulence.

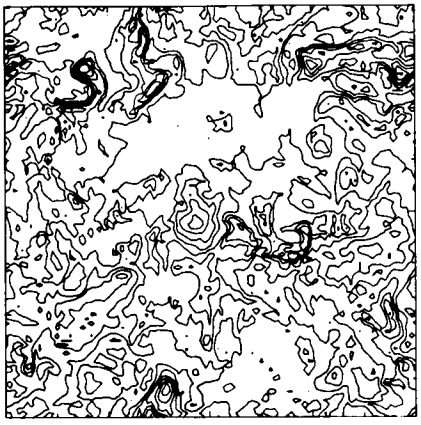

Fig. 13(b) Density contours.

Navier-Stokes Simulations for Hypersonic Low-Density Flows

For an accurate prediction of the aerothermal environment of a space vehicle entering the Earth's atmosphere in the high-altitude (low-density) flight regime, the multicomponent nonequilibrium gas chemistry, as well as the surface slip effects, must be included in modeling the flow field. Such rarefied and highly energetic flows are of particular interest for current and future space transportation systems. Recent numerical simulation studies have been performed in which the Navier-Stokes (N-S) equations were used to model chemical nonequilibrium flows with multicomponent surface slip boundary conditions. These solutions are applicable along the stagnation streamline of a blunt nose tip at low-density hypersonic flow conditions. The governing equations are highly nonlinear and are solved by a numerical finite-difference method known as Successive Accelerated Replacement (SAR).

The comparison of the N-S stagnation-point heat-transfer results with those obtained with the direct simulation Monte Carlo (DSMC) method (a particle approach) provides an indication of the applicability of continuum methods to low-density hypersonic flows. Also shown are the continuum viscous shock-layer (VSL) results without either surface or shock slip boundary conditions. The VSL data begin to depart from the DSMC results for free-stream Knudsen numbers (λ_∞/R_N where λ_∞ is the undisturbed mean free path length and R_N is the nose radius, which is 1.3 m) of about 0.03. The departure is rapid for the VSL results. The departure of the N-S results without surface slip is less rapid because the N-S simulation included the shock wave structure by integrating all the way to free-stream conditions and also because it contains higher order terms than the VSL equations. Finally, the N-S solution with surface slip provides good agreement with the DSMC heat-transfer calculations for free-stream Knudsen numbers as large as unity. The three methods are in good agreement at an altitude of 92.35 km. For altitudes less than 92.35 km, the results from the N-S and VSL methods compare well.

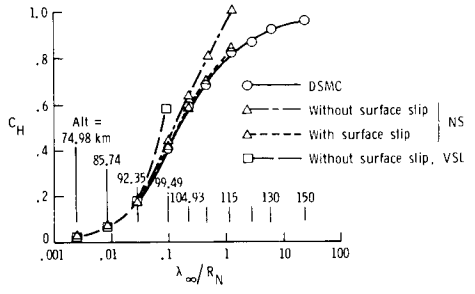

Fig. 14 Heat transfer coefficient versus Knudsen number.

Structural Behavior of the Space Shuttle SRM Tang-Clevis Joint

The space shuttle Challenger accident investigation focused on the failure of a tang-clevis joint on the right solid rocket motor (SRM). The existence of relative motion between the inner arm of the clevis and the O-ring sealing surface on the tang has been identified as a potential contributor to this failure. This motion can cause the O-rings to become unseated and therefore lose their sealing capability. Finite-element structural analyses have been performed where particular attention has been paid to modeling concerns such as mesh discretization and contact of the joint components. To model the details of the contact between tang, pin, and clevis and also to predict the general three-dimensional stress state in the joint, three-dimensional elastic, solid finite elements were selected for the analysis. The elements have elastic material properties for all analyses performed in this study. These computations were carried out via remote link with the Cray XMP-12 and XMP-48 sited at Ames Research Center. Further analyses of the nonlinear shell problem for the complete booster are being performed on the Cray-2.

A key ingredient of the joint modeling approach is the method used for connecting the separate finite element models of the tang, clevis, and pin. It was recognized from the outset that the contact regions between these components would change as a function of loading, leading to a nonlinear analysis problem. This nonlinearity

occurs, for example, when a gap that exists between unloaded components closes when loaded. The actual contact is modeled by adding a nonlinear spring between two adjacent contact nodes. The nonlinear spring stiffness curves are piecewise-linear functions of the relative displacement and are generated, for example, such that a high stiffness results for any compression of the spring and a low or zero stiffness results if the spring stretches.

Following the accident, structural tests ("referee tests") at Morton-Thiokol Incorporated were designed to gain a better understanding of the deflection behavior of the tang-clevis joint and to aid in the verification of analytical models. The test article consisted of a case segment tang joined to a case segment clevis; domed end closures seal the ends of the two-segment test article. This assembly was tested under hydrostatic pressure from zero to 1004 psi.

The finite-element model of a one-degree slice of the original SRM joint used in the comparisons is shown on Figure 15. For the baseline analysis case, no clearance around the pin is assumed. High contact forces develop around the pin under the pressure load. Even with a low coefficient of friction, these contact forces are sufficient to prevent the tang and clevis arms from sliding along the pin. The applied loading is 1000 psi internal pressure which is assumed to act on the surfaces of the tang and inner clevis arm and all surfaces of the primary O-ring groove. This loading condition implies that the primary O-ring forms a seal at the downstream corner of the O-ring groove.

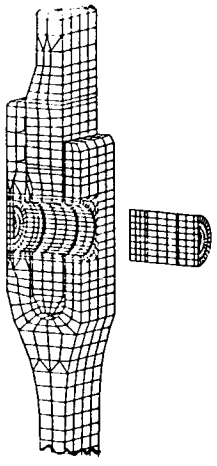

Fig. 15 Finite element model of local joint (4405 nodes and 2868 elements).

A comparison of deflections from the referee test and analysis is shown in Figure 16. These deflections have been exaggerated in the deformed geometry plot. Agreement between test and analysis for the relative tang and clevis motions in the joint itself as indicated by the results on Figure 16 is generally good. Gap motion midway between the two O-ring grooves is measured in the referee tests using eight displacement transducers located around the circumference of the case. The measured values of gap motion ranged from 0.035 to 0.041 inches with an average value of 0.037 inches for a 1000 psi pressure loading. As shown in Figure 16, the predicted value of the gap motion is approximately 17% below this average measured value. The close-up view of the deformed geometry qualitatively indicates the severity of the pin bending due to the bearing forces and the tang rotation.

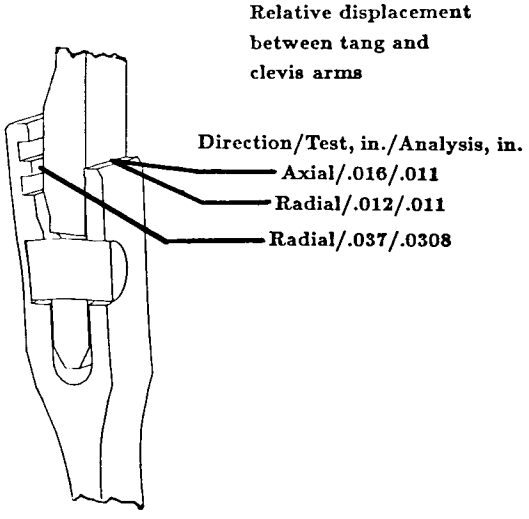

Fig. 16 Deformed geometry (exaggerated deflections).

The largest stress values occur in the joint itself in the vicinity of the pin. The pin contacts the tang at the lower edge of the tang hole and at the upper edges of the clevis holes. High compressive stresses are present in these locations and many of the stresses substantially exceed yield values for both the D6AC case material (180 ksi) and the MP35N pin material (250 ksi).

These analyses have demonstrated the difficulty of accurately predicting the structural behavior of the tang-clevis joint. Stresses in the vicinity of the connecting pins, obtained from elastic analyses, considerably exceed the material yield allowables indicating that inelastic analyses are probably necessary. Parametric variation of pin-hole taper, used to approximate the inelastic behavior of deformations in the tang hole, agreed with the measured gap motions.

Three-Dimensional Stress Analysis of Cracked or Uncracked Structures

Three-dimensional, elastic and elasto-plastic, finite-element codes for analysis of structures with or without cracks have been developed at NASA Langley. Advanced finite-element formulations are coupled with highly vectorized computer codes for use on the VPS-32 supercomputer.

Finite-element formulations using 8- or 20-noded isoparametric hexahedron elements are used for stress analyses of cracked or uncracked structures. For cracked elastic structures, a square-root singularity is incorporated around crack fronts. The strength of the singularity (the stress-intensity factor) is calculated for various

crack sizes and shapes in common aircraft components, such as surface cracks emanating from rivet holes. The stress-intensity factors are used to predict the fatigue life and fracture strength of damaged aircraft structures. For elastic-plastic materials, the fatigue-crack growth and fracture processes are simulated on the computer to better understand the mechanism of fatigue-crack growth and to develop improved fracture criteria. This code was recently used in analyzing the influence of plastic yielding on the performance of a solid-rocket booster joint. For uncracked structures, the programs are used to obtain accurate stress distributions in complicated structures, such as the shear-stress distributions around pin holes in a wooden wing-tunnel blade, as shown in Figure 17. The model of the lower half of the blade was composed of 3,300 (20-noded) elements and had about 50,000 degrees of freedom. The program PATRAN was subsequently used to reduce the enormous amount of data to color plots showing the stresses in the most highly stressed regions of the blade. The dark regions in the slice taken from the wooden hub show the most highly stressed regions around the pin-loaded holes. (The color plots show distribution of stresses within the dark regions.) The maximum shear stress was 1400 psi. The finite-element code was used to analyze a redesigned blade, with a smoother transition from the blade to hub region, and the results showed a 30% reduction in maximum stress.

The application of three-dimensional stress analyses to both cracked and uncracked structures will significantly enhance certainty in stress distributions and may prevent many previously unanticipated failures. These computer codes will be made more accessible to other researchers by developing more friendly codes and user guides.

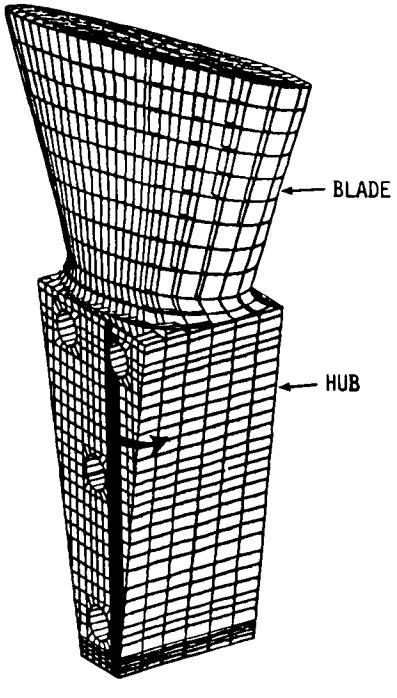

Fig. 17(a) Model of wood blade and hub.

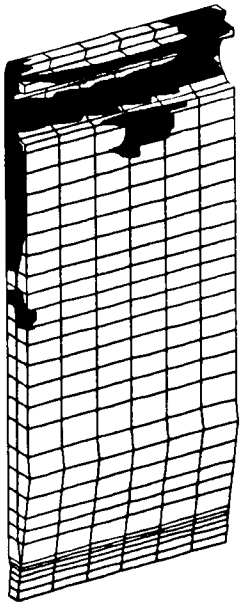

Fig. 17(b) Shear stress distribution around pin-loaded hole.

Integrated Interdisciplinary Optimization Procedure for Large Space Antenna Design

Previous work in optimizing large space antenna structures generally concentrated on minimizing root mean square (rms) surface distortions, thereby indirectly maximizing electromagnetic (EM) antenna performance. The present work involves a direct approach to maximizing EM performance while minimizing mass. Integrating the thermal, structural, and EM analyses in the context of an optimization procedure is an effective design approach because the influence of each type of response on the other is accounted for directly and automatically. A finite-element thermal analysis and structural deformation analysis program is combined with a NASA-Langley-developed electromagnetic radiation program and a standard optimization program. The system is used to perform a thermal analysis, transfer the temperatures to the structural model, and compute the deformed shape of the antenna reflector. The deformed shape in the EM analysis is used to determine performance parameters including peak gain, side lobe levels, beam width, pointing direction, and cross-polarization.

The procedure has been tested on a 55-m tetrahedral antenna reflector shown in Figure 18. A representative orbital position was chosen as the design point and a design was sought which minimized structural mass while attaining a peak gain of at least 19,000. The results of the optimization are shown in the lower part of Figure 18. Structural mass, rms surface distortion, and peak gain are shown for the initial design and for the first three design cycles. Design goals are essentially achieved at the third cycle. The contour plots show the evolution of surface distortion as the design is improved.

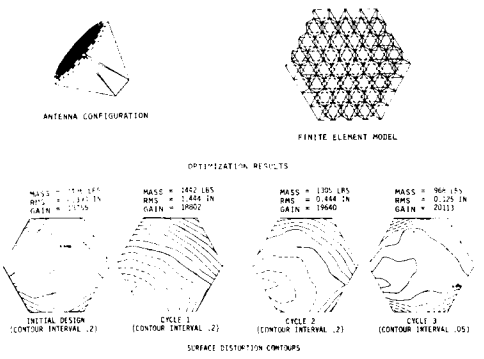

Fig. 18 Application of optimization procedure to space antenna design.

Solid lines are displacements toward the feed, and dashed lines are displacements away from the feed. Initially, there is a deep valley in the reflector, but at the end of the third cycle, the distortion is much smaller, and the reflector shape is nearly a perfect paraboloid as required. The remaining distortion occurs near the outer edges, which are not as important to EM performance as the center because of feed taper.

Concluding Remarks

Computational analysis at Langley Research Center covers a wide range of aerospace research disciplines, and is crucial to our interdisciplinary research goals. The demand for supercomputing resources seems unlimited, spurred by the quantity and quality of information now derived from the results. This paper attempts to convey the scope of computational research and advanced applications at Langley by showing some examples from several areas: Aerodynamics, fluid dynamics, hypersonics, structures, and optimization of space systems. Areas which were not shown, but which are important elements of our program, include atmospheric dynamics modeling; quantum physics computations related to materials characterization; and severe storm downburst computations in support of wind-shear prediction and avoidance.